

Electron and ion heating, acceleration and energy partition during magnetic reconnection

J. F. Drake University of Maryland

J. Dahlin University of Maryland

C. Haggerty University of Delaware

T. D. Phan UC Berkeley

M. A. Shay University of Delaware

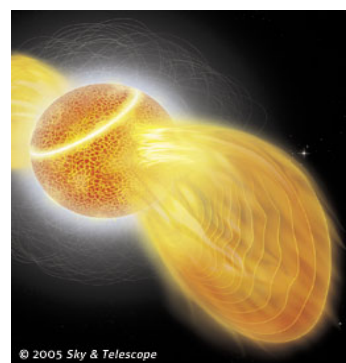
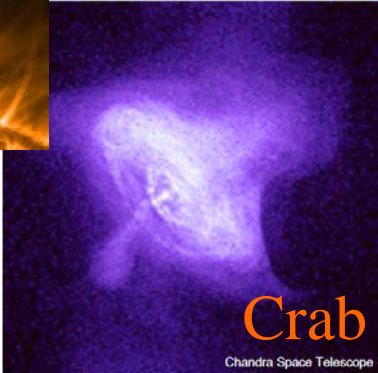
M. Swisdak University of Maryland

Magnetic Energy Dissipation in the Universe

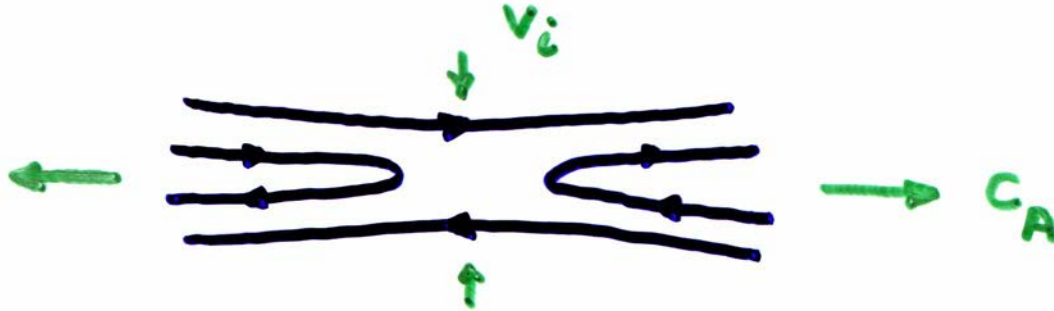
- Magnetic reconnection is the dominant mechanism for dissipating magnetic energy in the universe
- The conversion of magnetic energy to heat and high speed flows underlies many important phenomena in nature
- Known systems are characterized by a slow buildup of magnetic energy and fast release
- A significant fraction of the released magnetic energy goes into energetic particles

Astrophysical reconnection

- Solar and stellar flares
- Pulsar magnetospheres, winds, PWNe
- AGN (e.g., blazar) jets, radio-lobes
- Gamma-Ray Bursts (GRBs)
- Magnetar flares

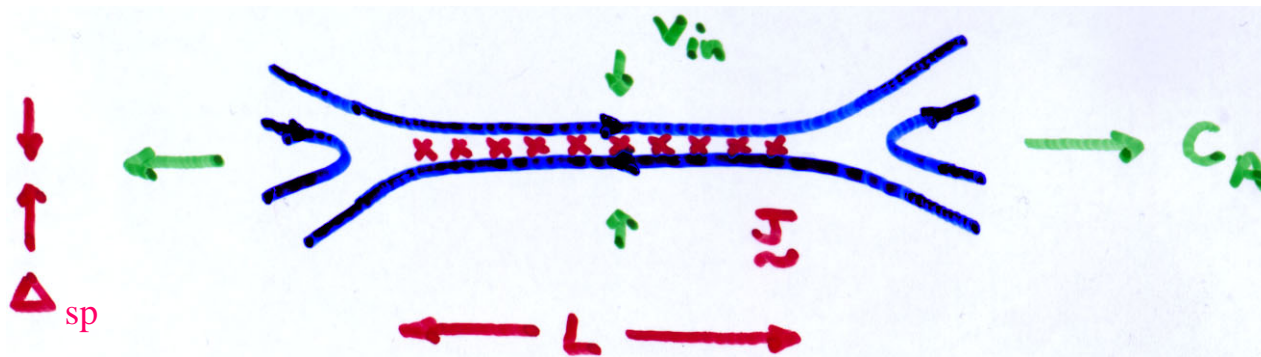


Magnetic Reconnection Basics



- Reconnection is driven by the magnetic tension in newly reconnected field lines
 - Drives outflow at the Alfvén speed c_A
 - Pressure drop around the x-line pulls in upstream plasma
- Dissipation required to break field lines
 - At small spatial scales since dissipation is weak
- Reconnection is self-driven
 - No external forcing is required

Classic Resistive MHD Description



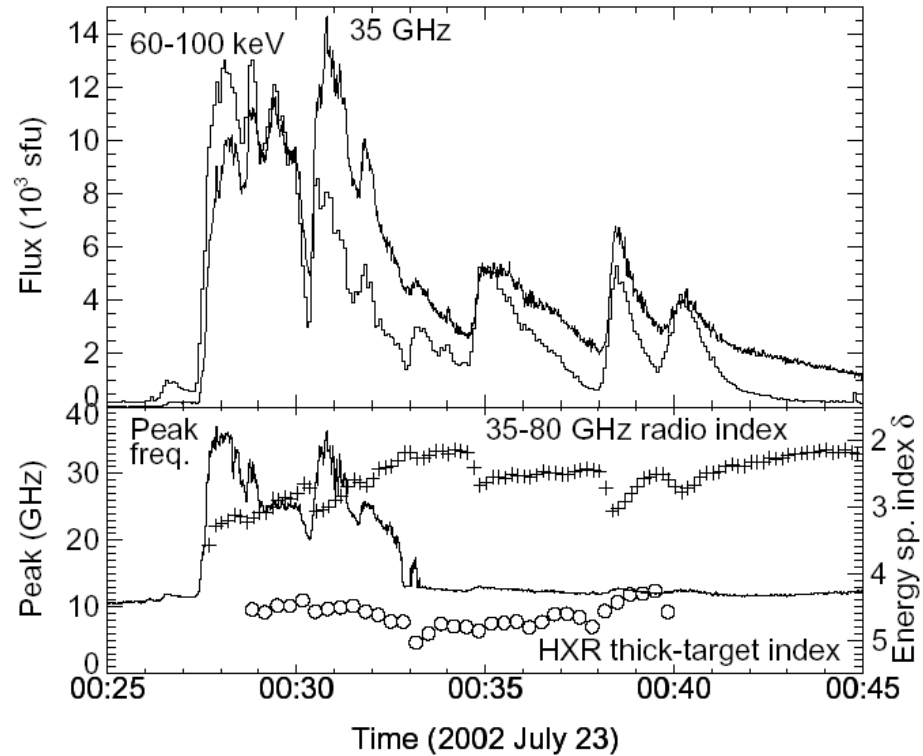
- Formation of macroscopic Sweet-Parker layer

$$V_{in} \sim (\Delta_{sp}/L) C_A \sim (\tau_A/\tau_r)^{1/2} C_A \ll C_A$$

- Slow reconnection
 - not consistent with observations
- Macroscopic nozzle
- Sensitive to resistivity

Impulsive flare timescales

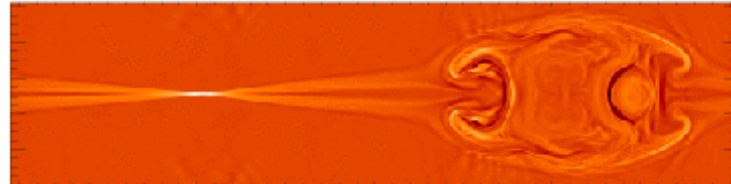
- Hard x-ray and radio fluxes
 - 2002 July 23 X-class flare
 - Onset of 10' s of seconds
 - Duration of 100' s of seconds.



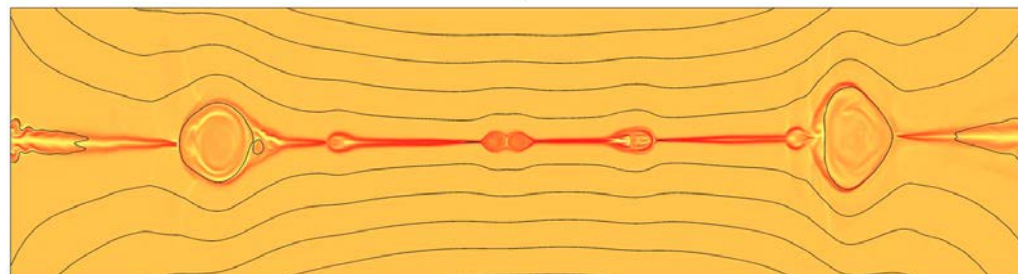
RHESSI and NoRH Data
(White et al., 2003)

Mechanisms for the fast release of magnetic energy: insensitive to dissipation

- Hall reconnection: an open Petschek-like outflow exhaust produces fast reconnection (Shay et al '99, Birn et al '01)

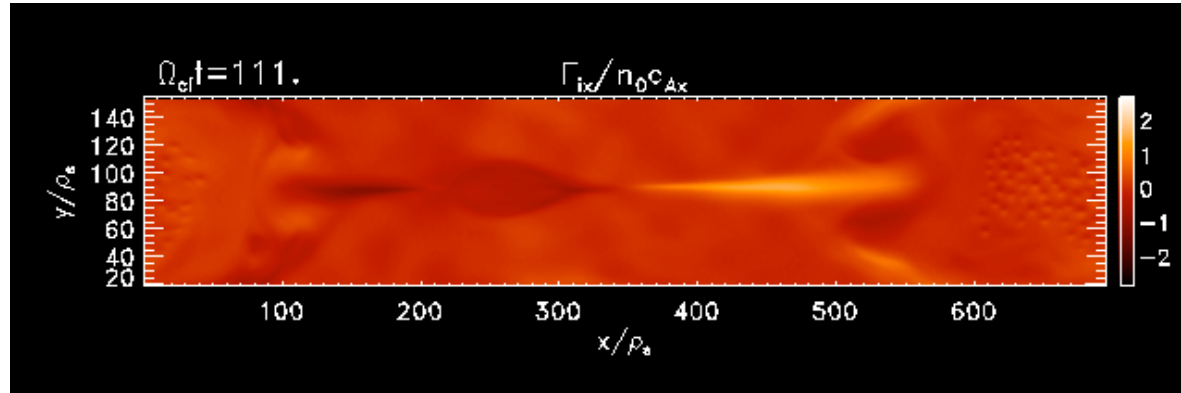


- Multi-island reconnection (Daughton et al '09, Bhattacharjee et al '09, Cassak et al '09)
 - Large-scale current layers break up into secondary islands



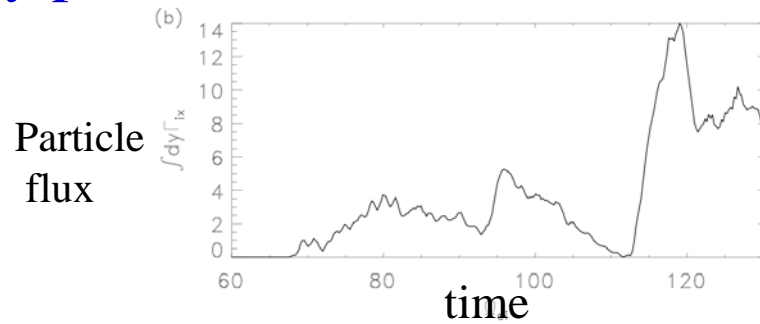
Multi-island reconnection

- Large-scale current layers break up into secondary islands



- Secondary islands carry particles out of the current layer

- Bursty reconnection

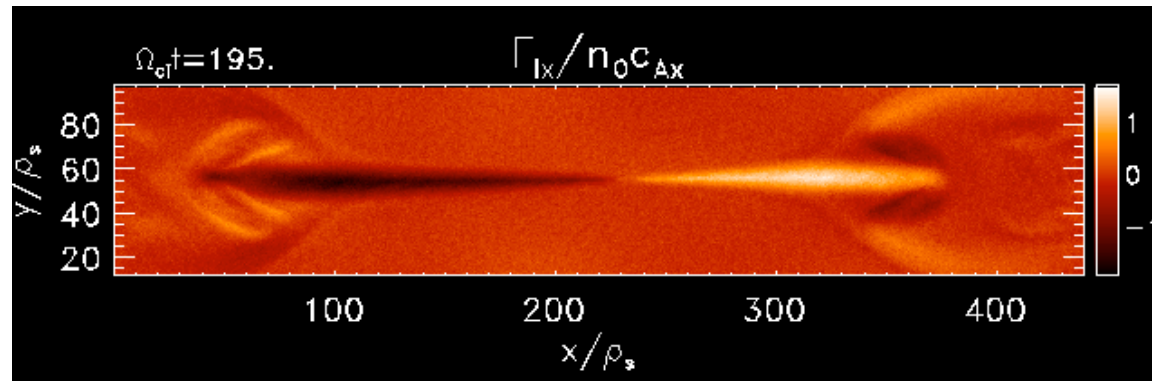


- Where?

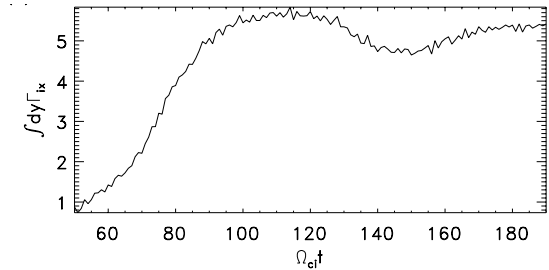
- Low resistivity MHD: $S = \tau_r/\tau_A > 10^4$ – solar corona?
 - Pair plasma
 - Collisionless: strong guide magnetic field at low β – solar corona?

Hall Reconnection

- Any system with dispersive waves at small scales produces an open exhaust and fast reconnection independent of dissipation (Birn et al '01, Rogers et al '01)
 - Whistler or kinetic Alfvén waves
 - Signature quadrupolar Hall magnetic field has been documented in the magnetosphere and laboratory

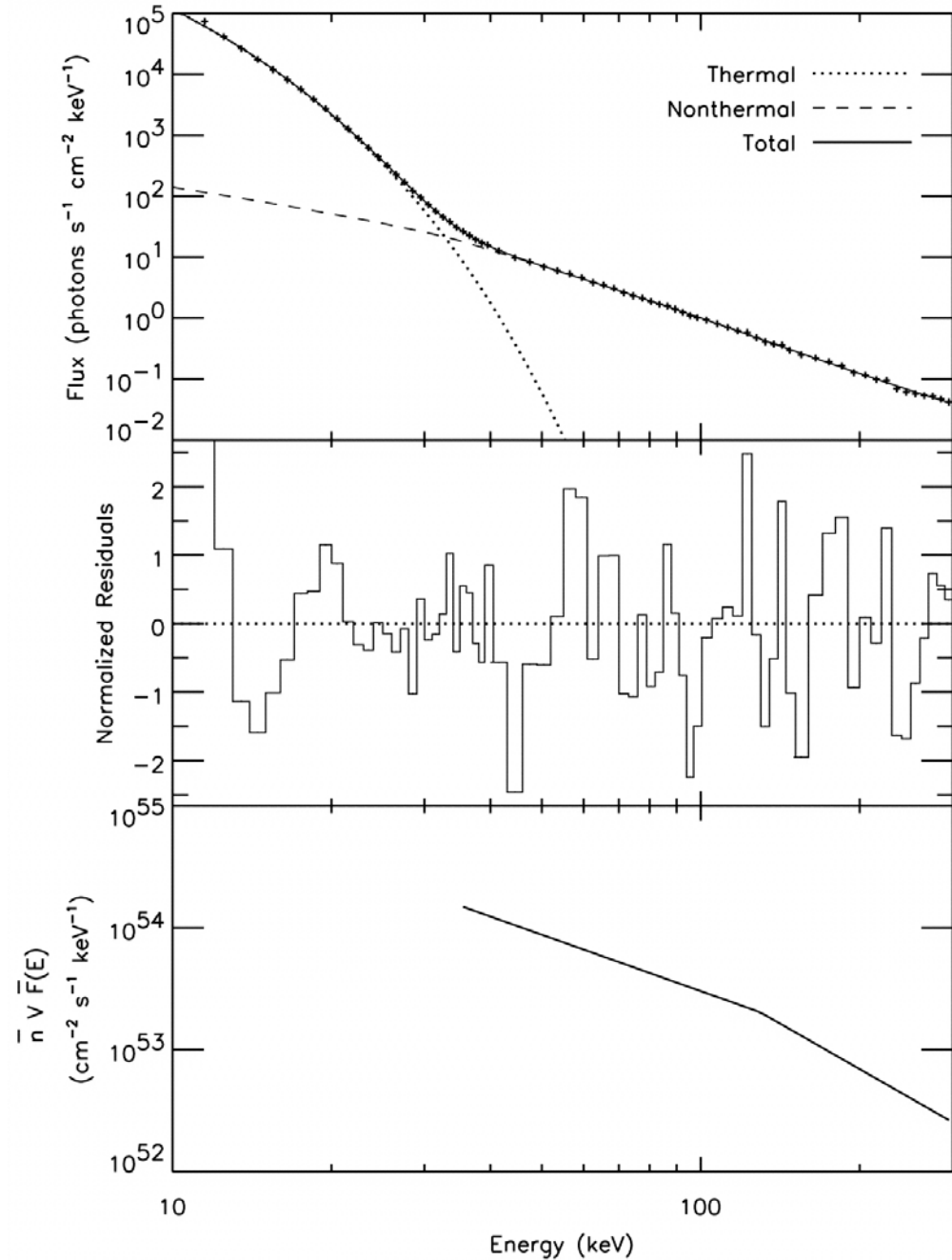


- Particle flux from the current layer is steady
- Collisionless regime except high guide field and low β

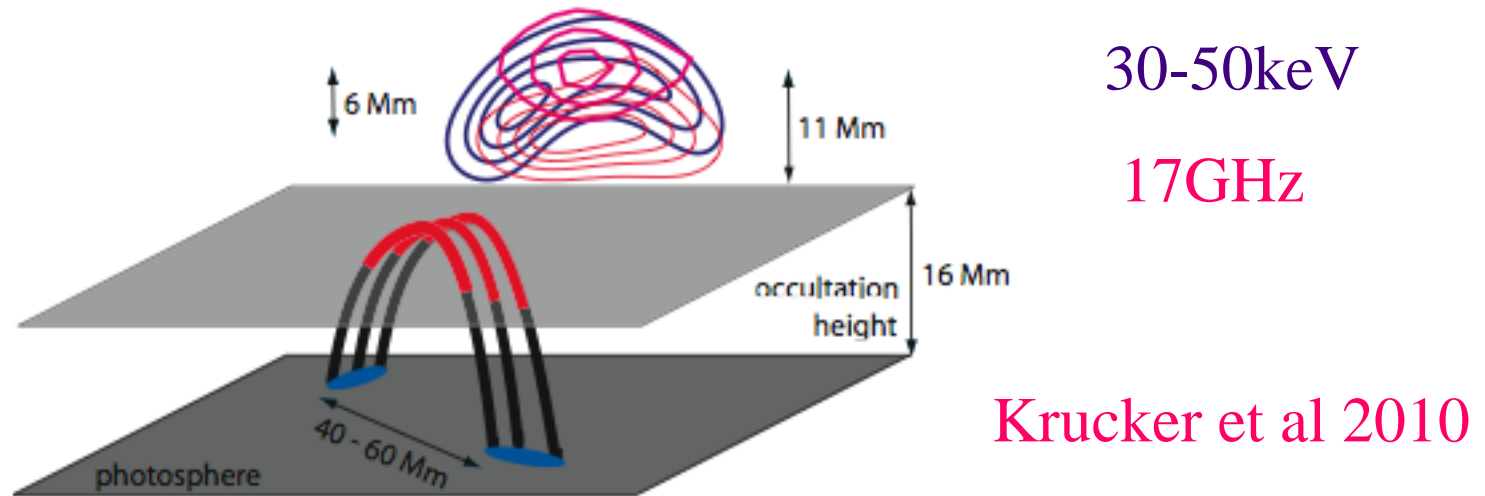


RHESSI observations

- July 23 γ -ray flare
(Holman, *et al.*, 2003)
- Double power-law fit
with spectral indices:
1.5 (34-126 keV)
2.5 (126-300 keV)



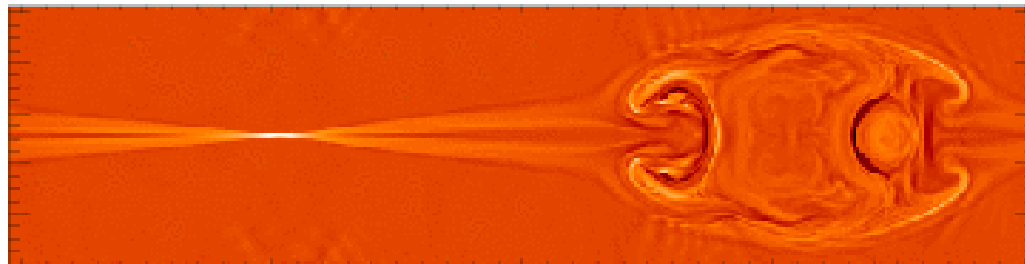
RHESSI occulted flare observations



- Observations of a December 31, 2007, occulted flare
 - A large fraction of electrons in the flaring region are part of the energetic component (10keV to several MeV)
 - The pressure of the energetic electrons approaches that of the magnetic field
 - Remarkable!

Energy release during reconnection

- The change in magnetic topology for reconnection takes place in the “diffusion” region
 - A very localized region around the x-line
 - This is not where significant magnetic energy is released



- Energy release primarily takes place downstream of the x-line where newly-reconnected field lines relax their tension
- Mechanisms for particle heating and energization can not be localized in the “diffusion region”

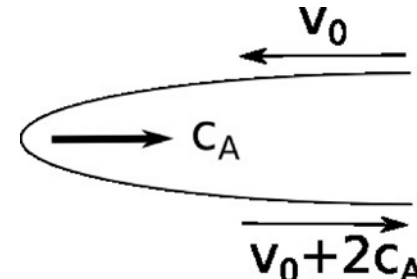
Basic mechanisms for particle energy gain during reconnection

- In the guiding center limit

$$\frac{d\varepsilon}{dt} = qv_{\parallel}E_{\parallel} + q\vec{v}_c \bullet \vec{E} + \mu \frac{\partial B}{\partial t} + q\vec{v}_B \bullet \vec{E}$$

- Curvature drift
 - Slingshot term (Fermi reflection) increases the parallel energy

$$v_c = \frac{v_{\perp}^2}{\Omega} \vec{b} \times (\vec{b} \bullet \vec{\nabla} b)$$



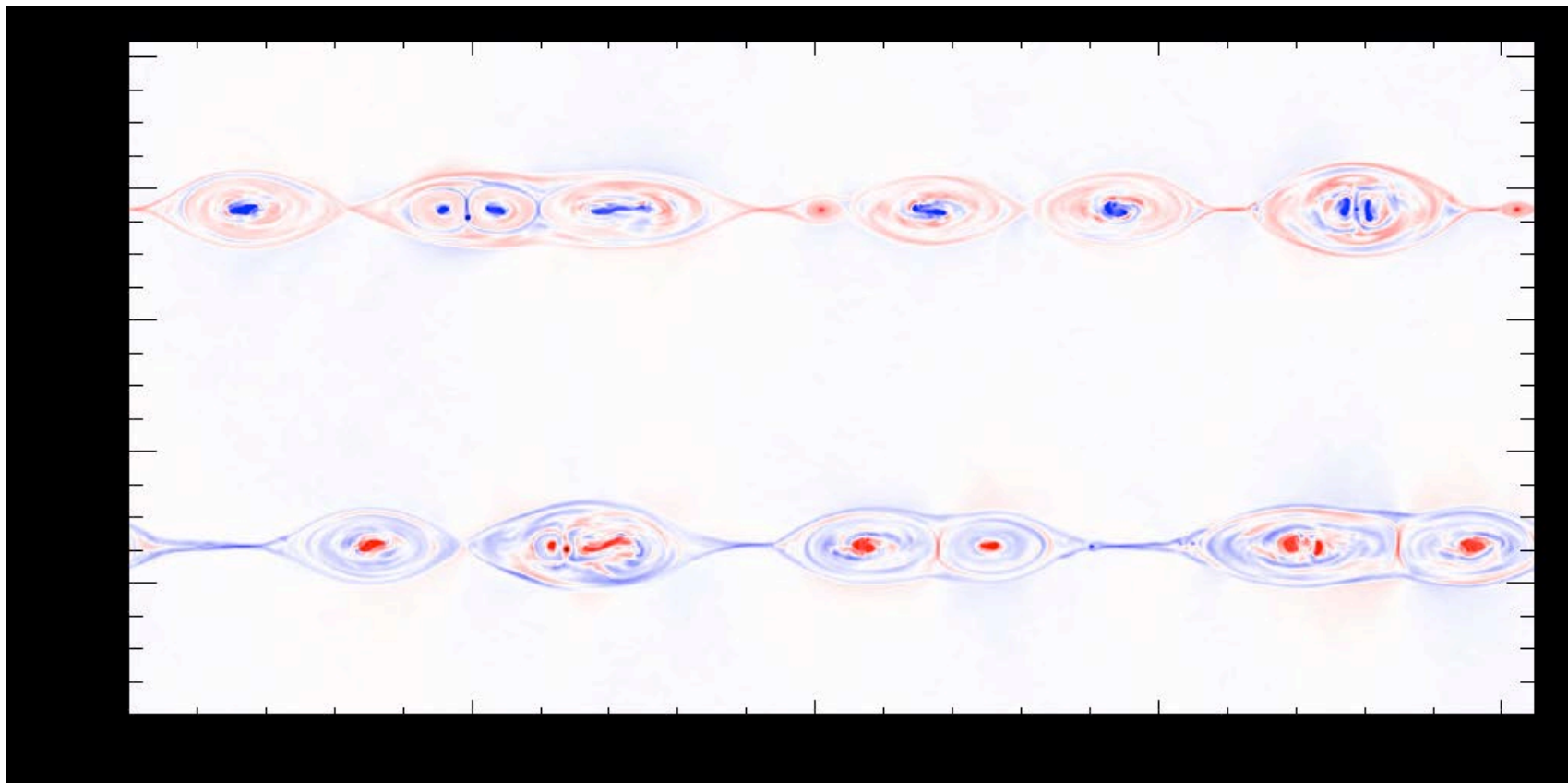
- Grad B drift
 - Betatron acceleration increases perpendicular energy – μ conservation

$$v_B = \frac{v_{\perp}^2}{2\Omega} \vec{b} \times \frac{\vec{\nabla} B}{B} \quad \mu = \frac{mv_{\perp}^2}{2B}$$

Electron heating during reconnection

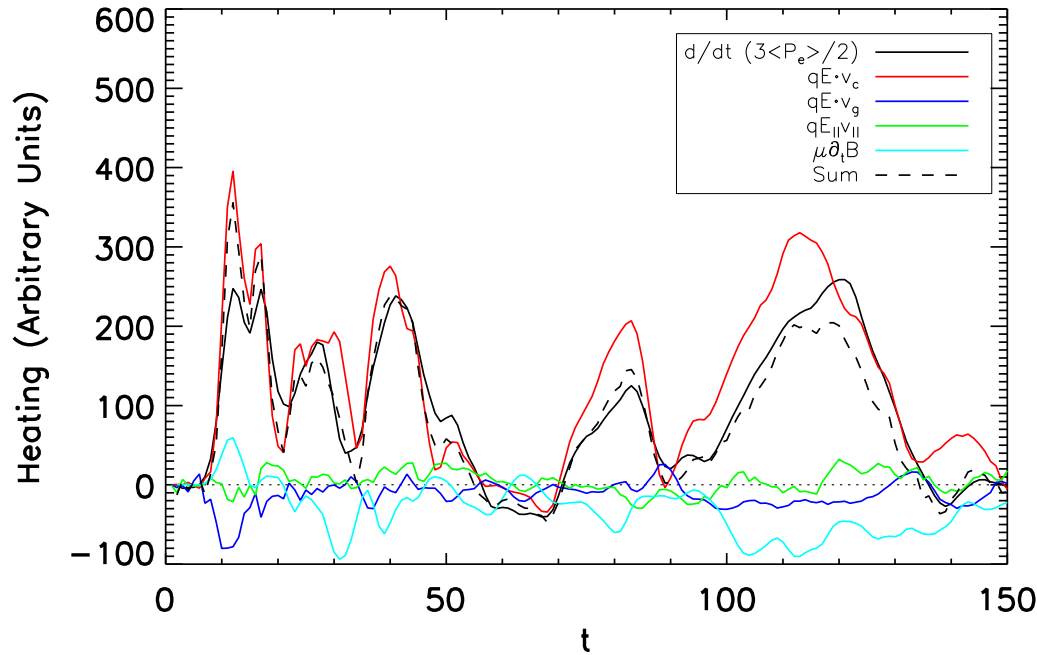
- Carry out 2-D PIC simulations of electron-proton system with a weak and strong guide fields (0.2 and 1.0 times the reconnection field)
 - $819.2d_i \times 409.6d_i$
 - Compare all of the heating mechanisms
 - Dahlin et al '14

$$d_i = \frac{c}{\omega_{pi}}$$



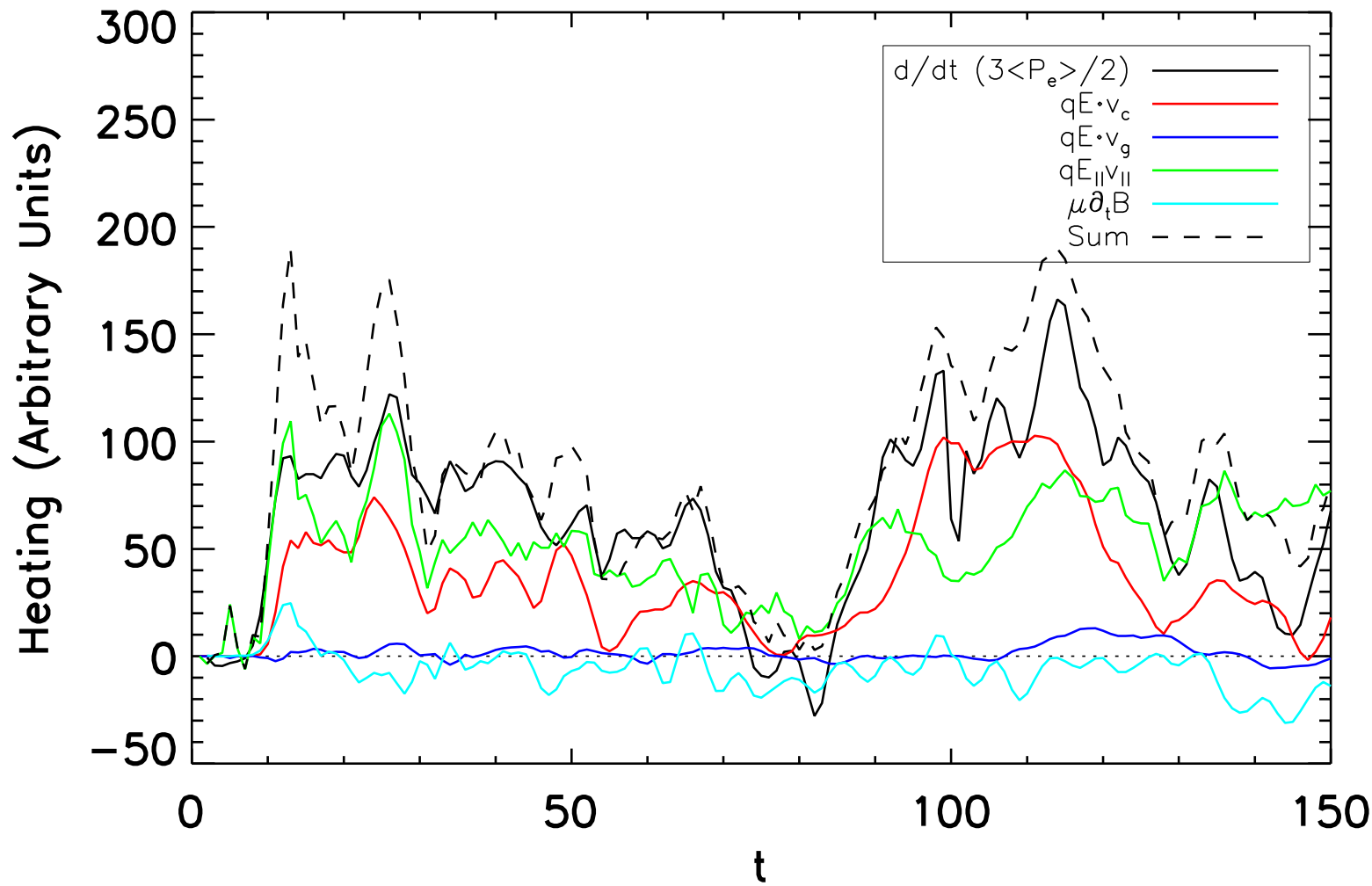
Electron heating mechanisms: weak guide field

- Slingshot term dominates (Fermi reflection)
- Parallel electric field term small – a surprise
- Grad B term is an energy sink
 - Electrons entering the exhaust where B is low lose energy because μ is conserved.



Electron heating mechanisms: strong guide field

- Fermi and parallel electric field term dominate
 - Longer current layers where $E_{\parallel} \neq 0$ with a guide field



Spatial distribution of heating rate from Fermi reflection

- Electron heating rate from Fermi reflection
 - Fills the entire exhaust
 - Not localized to narrow boundary layers
 - Traditional fluid picture of energy cascade to small scales and dissipation does not apply

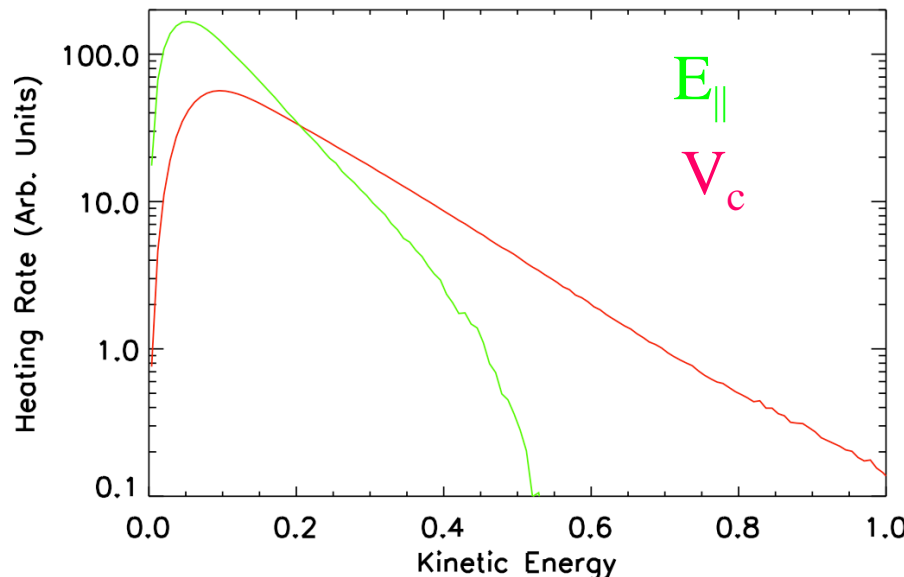
Acceleration mechanism for highest energy electrons

- Fermi reflection dominates energy gain for highest energy electrons

– Where $v_c \sim v_{\parallel}^2$

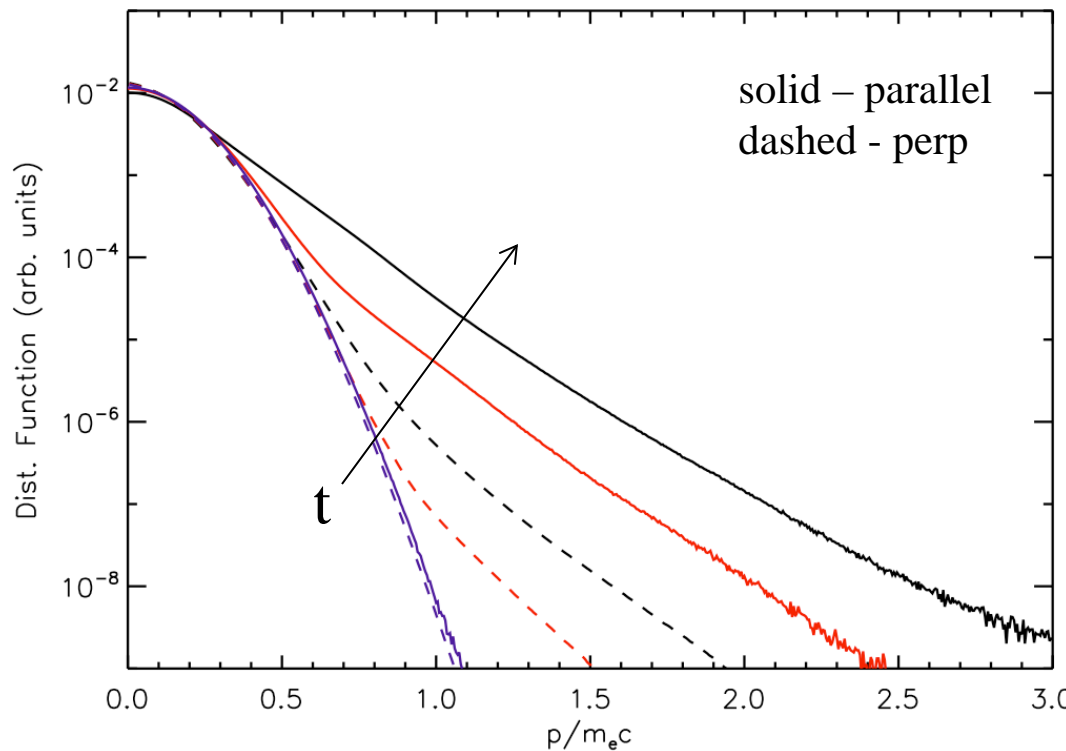
$$\frac{d\varepsilon}{dt} \sim qv_{\parallel}E_{\parallel} + q\vec{v}_c \bullet \vec{E}$$

- Recent simulations of pair and relativistic reconnection also see the dominance of Fermi reflection (Guo et al '14, Sironi and Spitkovsky '14)



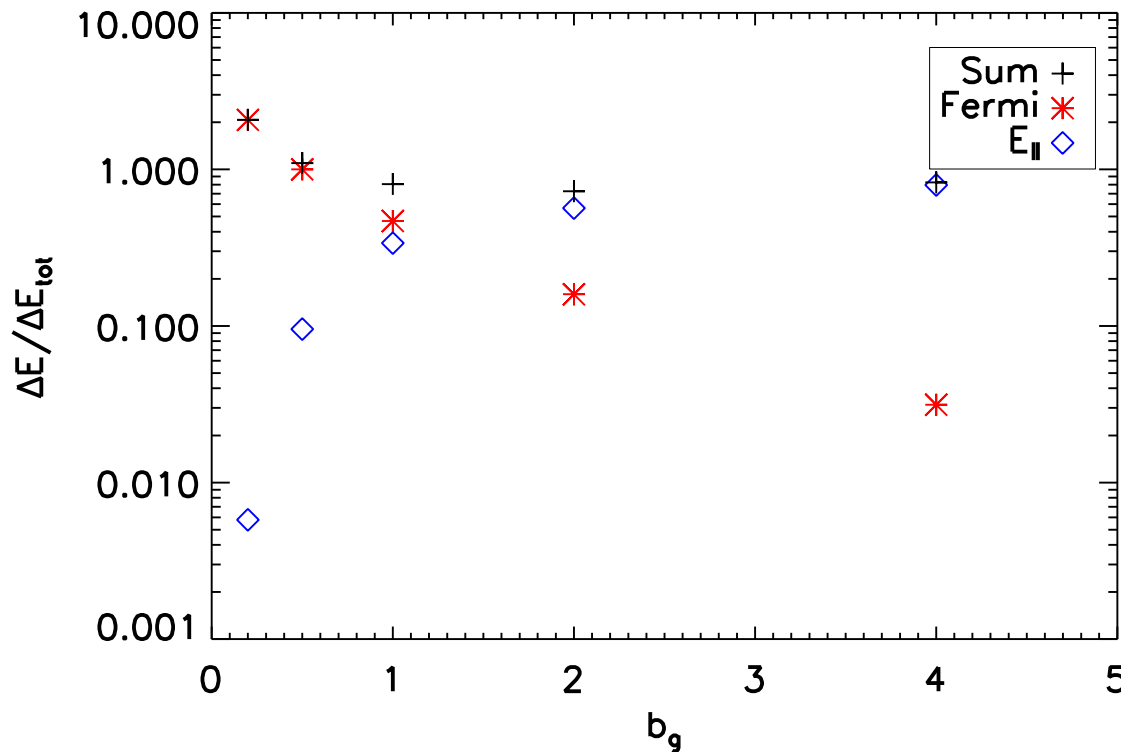
Electron spectral anisotropy

- The dominant acceleration mechanisms accelerate electrons parallel to the local magnetic field – Fermi slingshot and E_{\parallel}
 - Extreme anisotropy in the spectrum of energetic electrons
 - More than a factor of 10^2
 - What limits the anisotropy?



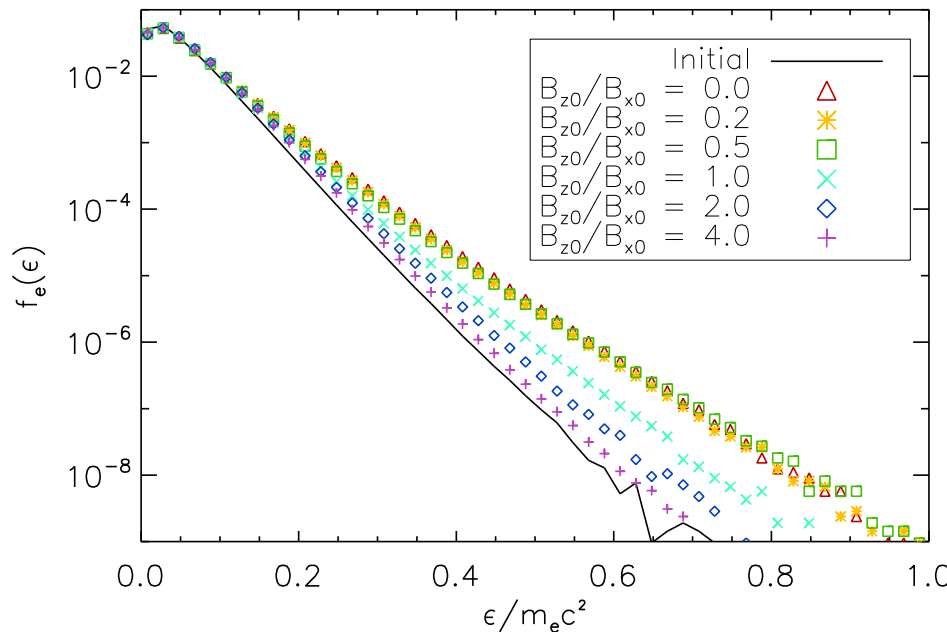
Transition to strong guide field reconnection

- Carried out a scaling study with guide field to determine electron acceleration mechanisms
- E_{\parallel} dominates for very strong guide field
 - Consistent with gyro-kinetic models?



Energetic particle spectra: guide field dependence

- Total electron heating insensitive to the guide field
 - Fermi dominates for weak guide field
 - E_{\parallel} dominates for strong guide field
- Energetic component strongly reduced in strong guide field limit
 - E_{\parallel} not an efficient driver of energetic electrons

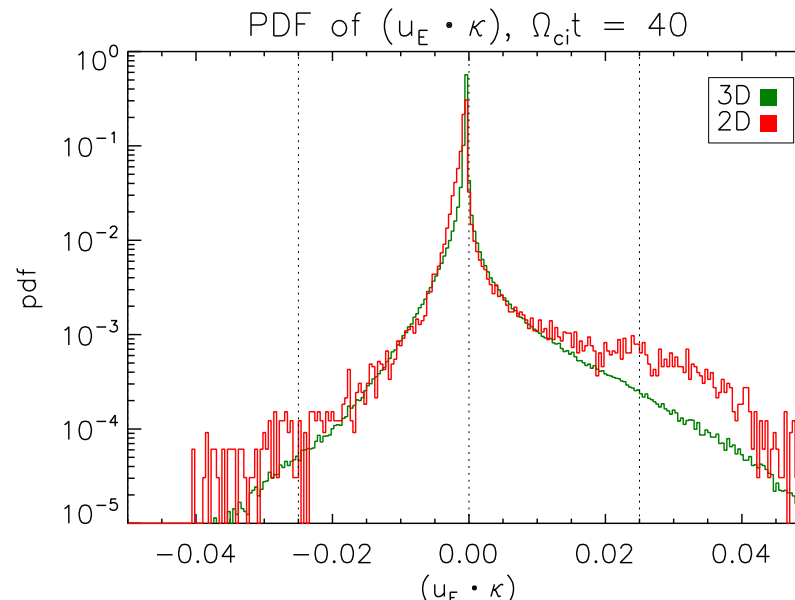
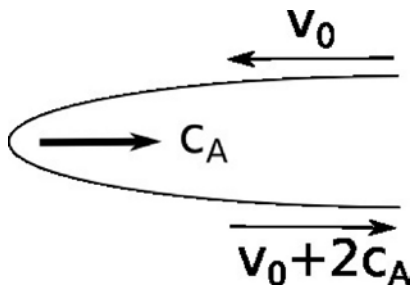


A measure of particle acceleration efficiency

- A measure of the rate of energy release and particle acceleration is the parameter

$$\vec{\kappa} \bullet \vec{V}_{ExB} = (\vec{b} \bullet \vec{\nabla} \vec{b}) \bullet \frac{c \vec{E} \times \vec{B}}{B^2}$$

- Dominantly positive in a reconnecting system and negative in a dynamo systems
- The dominance of positive values establishes that particle acceleration is a first order Fermi mechanism



Heating and the electron-ion energy partition during reconnection: weak guide field

Electron-ion Energy Partition: single x-line

- Where does the released magnetic energy go?
- Available magnetic energy per particle from Poynting flux

$$W_0 = \frac{1}{n_{up}} \frac{B_{up}^2}{4\pi} = m_i c_{Aup}^2$$

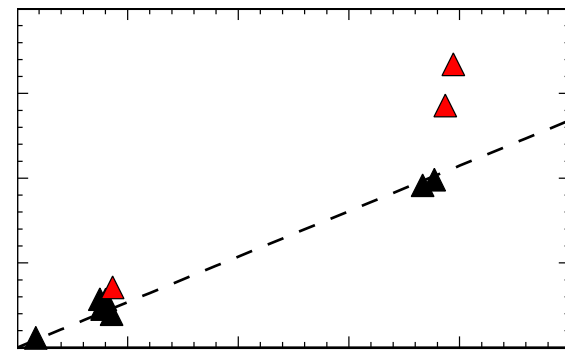
- Magnetopause enthalpy flux observations (Phan et al '13, '14)

$$\Delta W_i = \frac{5}{2} \Delta T_i = 0.33 W_0 \quad \Delta W_e = \frac{5}{2} \Delta T_e = 0.043 W_0 \quad \Delta W_{flow} = 0.5 W_0$$

- Parallel heating exceeds perpendicular heating
- Magnetotail observations (Eastwood et al '13)
 - Ions carry most of the released magnetic energy
 - Dominantly parallel heating
- MRX observations (Yamada et al '14)
 - Ions carry 2/3 and electrons 1/3 of the released energy

Scaling of electron and ion heating: simulations

- The partition of energy going to electrons and ions is not universal
 - Higher upstream electron pressure leads stronger electron heating (red triangles) and reduced ion heating. Why?
 - Total electron and ion heating is universal
- Total electron and ion heating matches magnetopause observations



$$\Delta(T_i + T_e) \sim 0.15 m_i c_A^2$$

Ion heating mechanism: single x-line

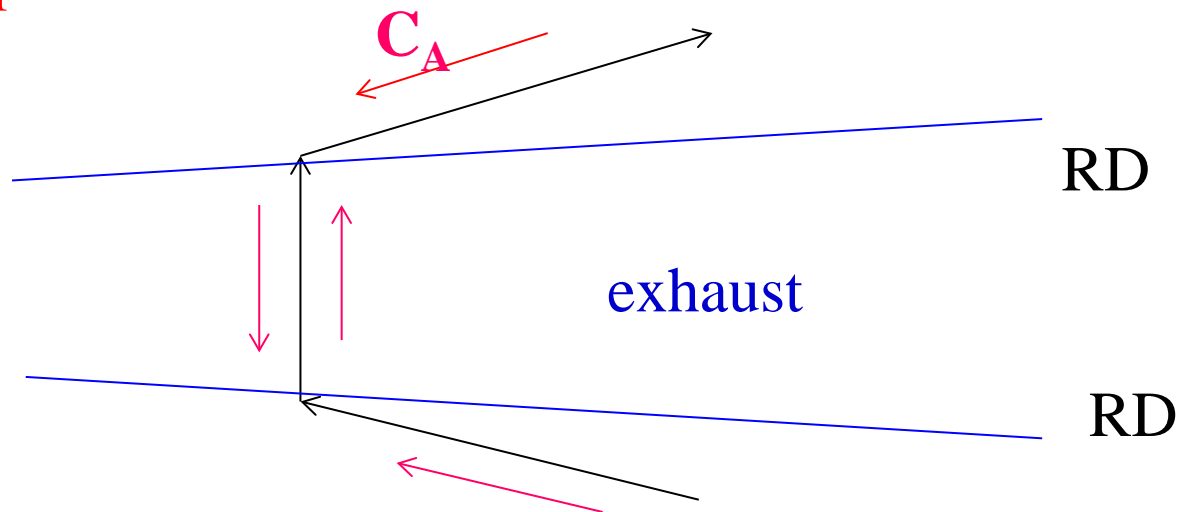
- Ion energy gain from Fermi reflection
 - leads to large parallel heating of ions
 - Measured throughout the magnetosphere
 - For $C_A \sim 2000 \text{ km/s}$ have $T_{\parallel} \sim 25 \text{ keV}$
- Measured scaling of ion temperature consistent with Fermi reflection (Phan et al 2014)

$$\Delta T_i \sim 0.13 m_i c_A^2$$

- Smaller than expected

$$\Delta T \sim \frac{1}{3} m_i c_A^2$$

Hoshino et al '98
Gosling et al '05
Phan et al '07

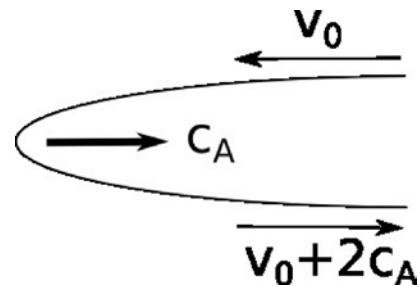


Electron heating mechanism: single x-line

- PIC simulations yield (Shay et al 2014)

$$\Delta T_e = 0.033 m_i c_A^2$$

- Same scaling as ions but less heating
- Single pass Fermi reflection $\sim m_e v_0 c_A$ is too small to explain observations and simulations
- How do the electrons gain so much energy?

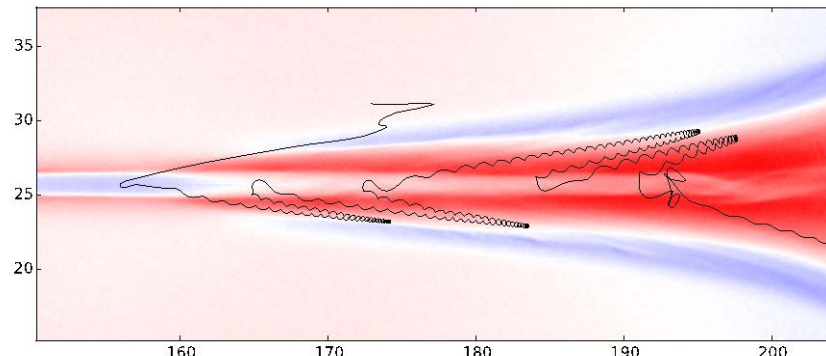


A large scale potential controls the relative heating of electrons and ions

- The development of a large scale potential boosts electron heating and suppresses ion heating
 - A large-scale potential develops to keep hot electrons in the exhaust from escaping upstream (Egedal et al '08)

$$\Delta\phi \sim T_e \ln \left(\frac{n_{exhaust}}{n_{up}} \right)$$

- The potential holds in electrons and enables them to undergo multiple Fermi reflections

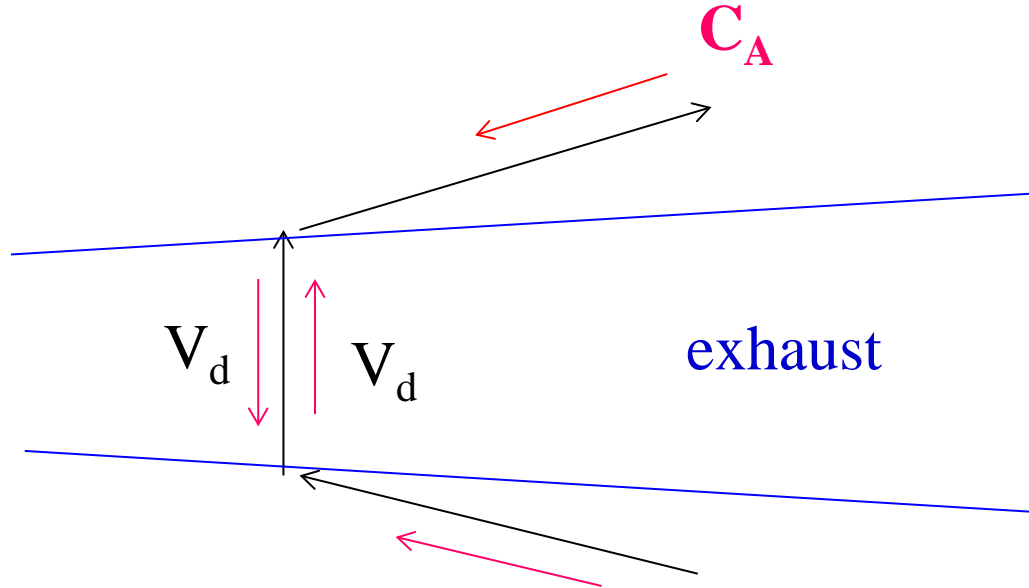


Haggerty et al 2105

The same potential suppresses ion heating

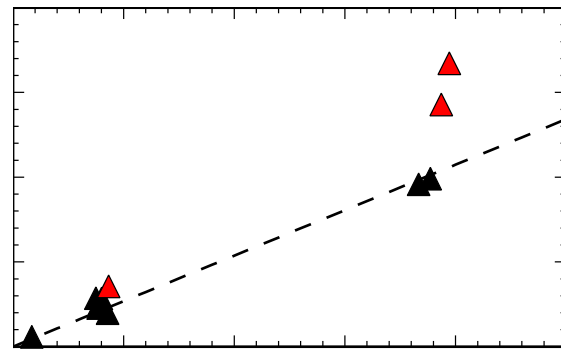
- In the frame of the exhaust ions move inward at C_A
- Ion velocity is reduced by the potential to V_d

$$\frac{1}{2}m_i V_d^2 = \frac{1}{2}m_i C_A^2 - e\varphi$$



Partition of electron and ion heating: simulations

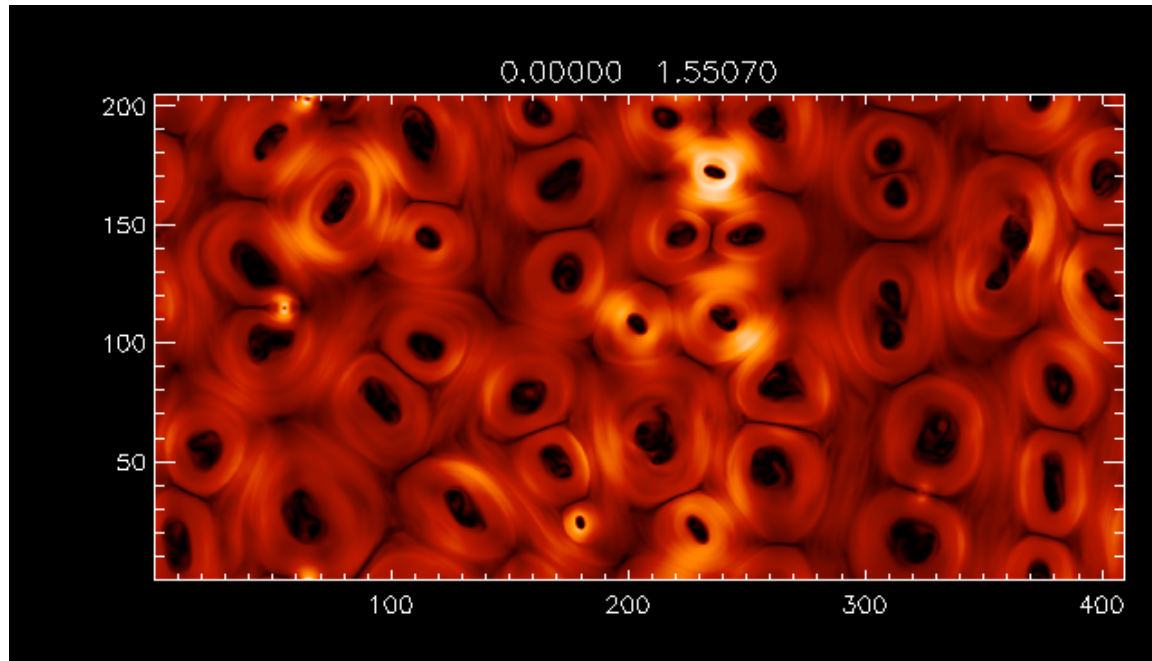
- The partition of energy going to electrons and ions is not universal
 - Higher upstream electron pressure leads to a higher potential and stronger electron heating (red triangles)
- Simulations match satellite observations of total electron and ion heating
 - Total electron and ion heating seems universal



$$\Delta T_e + \Delta T_i = 0.15 m_i c_{Aup}^2$$

Particle acceleration in multi-island reconnection

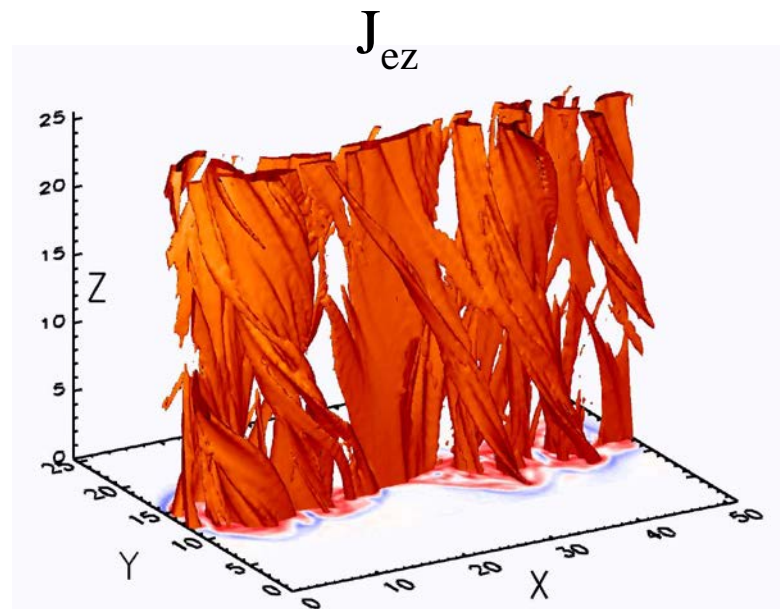
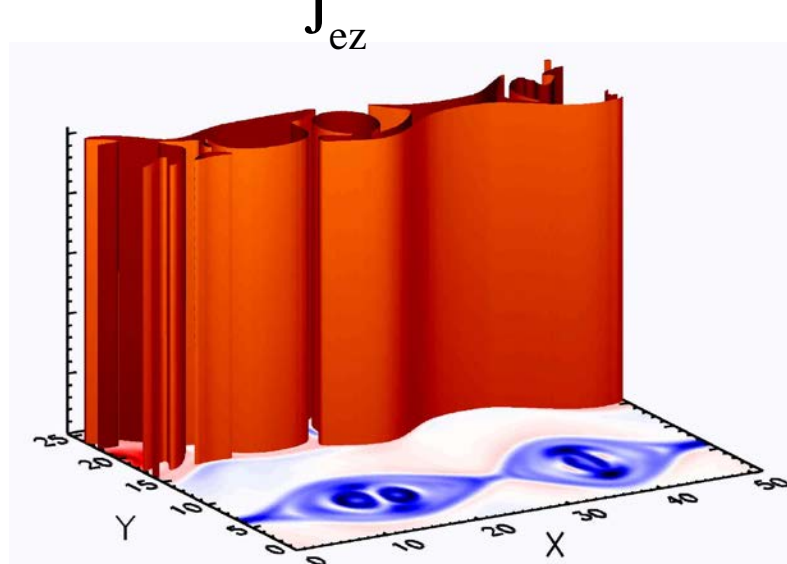
- Single x-line reconnection can not explain the most energetic particles seen in the magnetosphere and flares
 - The potential is too weak to contain the most energetic electrons
- Particles trapped in contracting and merging magnetic islands can undergo multiple Fermi reflections



Tajima and Shibata '97
Drake et al '06, '10, '13
Oka et al '10
Dahlin et al '14, '15
Guo et al '14, '15

Particle acceleration in 3D reconnection

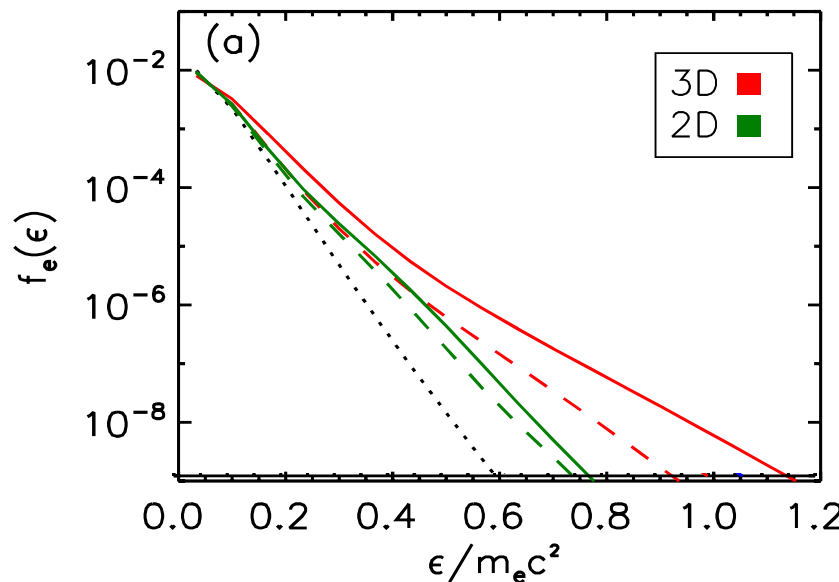
- In a 3D system with a guide field magnetic reconnection becomes highly turbulent (Daughton et al '11)
 - No magnetic islands
 - Chaotic field line wandering and associated particle motion
- What about particle acceleration?



Dahlin et al '15

Energetic electron spectra in 3D reconnection

- 3D simulation with domain size $102.4d_i \times 51.2d_i \times 25.6d_i$
- The rate of energetic electron production is greatly enhanced in 3D
 - The number of energetic electrons increases by more than an order of magnitude
 - The rate of electron energy gain continues robustly at late time with no evidence for saturation as in the 2D model. Why?



Impact of 3-D dynamics on particle acceleration

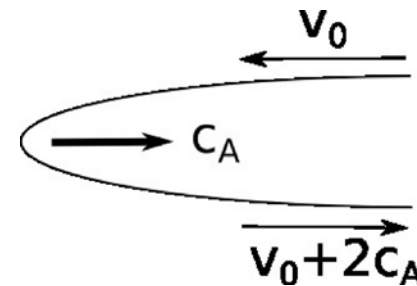
- In 3-D field lines can wander so particles are not trapped within islands
- Electrons gain energy anywhere in the reconnecting volume where magnetic field lines are locally relaxing their tension

Electrons with $\gamma > 1.5$

2D



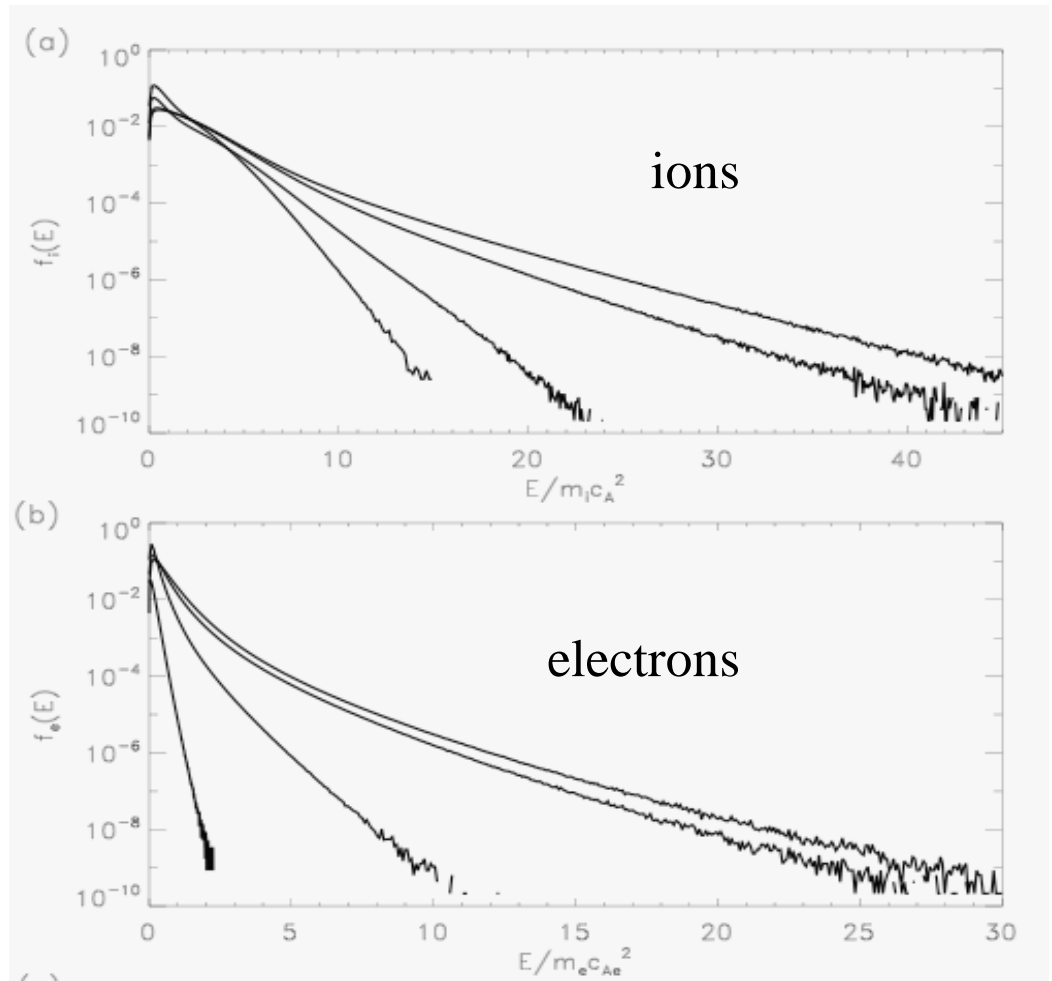
3D



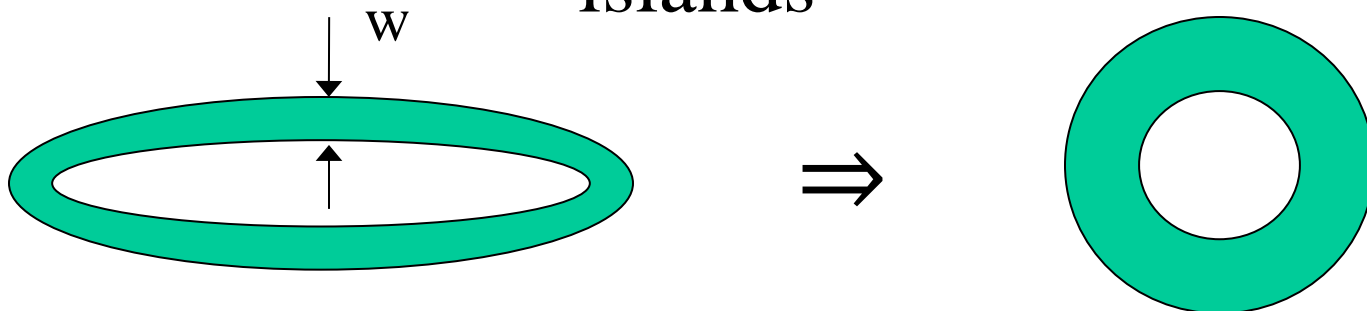
Dahlin et al '15

Electron and ion energy spectra

- Both ions and electrons gain energy through Fermi reflection in contracting and merging magnetic islands
- Develop a transport model to understand and describe how energetic particles are produced in a multi-island system



Fermi acceleration in contracting and merging islands



- Area of the island Lw is preserved
 \Rightarrow **nearly incompressible dynamics**
- Magnetic field line length L decreases
- Parker's transport equation
$$\frac{\partial F}{\partial t} + \nabla \bullet uF - \nabla \bullet \kappa \bullet \nabla F - \frac{1}{3}(\nabla \bullet u) \frac{\partial}{\partial p} pF = 0$$
 - Only compression drives energy gain. Why?
 - Parker equation assumes strong scattering \Rightarrow isotropic plasma
- Retaining anisotropy is critical for reconnection

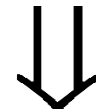
Energy gain in a bath of merging islands

- Total area preserved
- Magnetic flux of largest island is preserved
- Particle conservation laws
 - Magnetic moment $\mu = p_{\perp}^2 / 2mB$
 - Parallel action $p_{\parallel} L$
 - Field line shortening drives energy gain

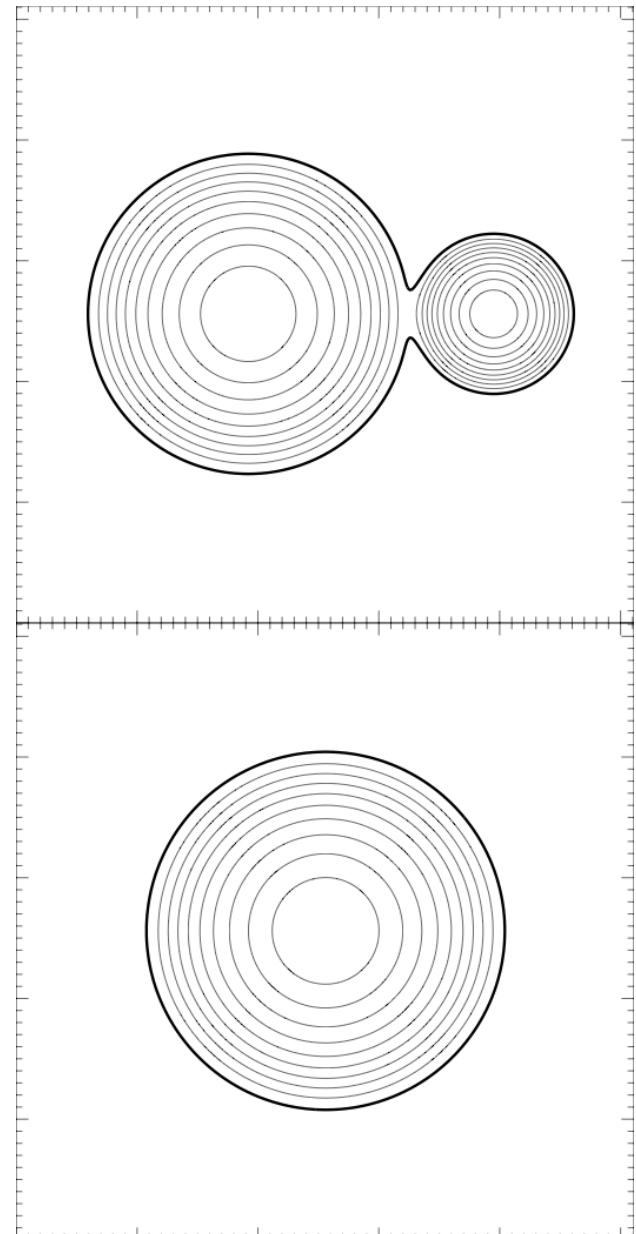
$$\frac{dp_{\parallel}^2}{dt} \sim 2 \frac{0.1c_A}{r_1 + r_2} p_{\parallel}^2$$



$$\frac{dp_{\perp}^2}{dt} \sim - \frac{0.1c_A}{r_1 + r_2} p_{\perp}^2$$



- No energy gain when isotropic



Particle acceleration in a multi-island reconnecting system

- Average over the merging of a bath of magnetic islands
- Kinetic equation for $f(p_{\parallel}, p_{\perp})$ with $\zeta = p_{\parallel}/p$
 - Equi-dimensional equation – no intrinsic scale
 - powerlaw solutions
 - Drake et al 2013

$$\frac{\partial f}{\partial t} + \vec{u} \bullet \vec{\nabla} f - \vec{\nabla} \bullet \vec{D} \bullet \vec{\nabla} f + R \left(\frac{\partial}{\partial p_{\parallel}} p_{\parallel} - \frac{1}{2p_{\perp}} \frac{\partial}{\partial p_{\perp}} p_{\perp}^2 \right) f - \gamma \frac{\partial}{\partial \zeta} (1 - \zeta^2) \frac{\partial}{\partial \zeta} f = 0$$

$$R \sim 0.1 \left\langle \frac{\alpha^{1/2} c_A}{r} \right\rangle \equiv \frac{1}{\tau_h} \quad \begin{matrix} \text{merging drive} & & \text{pitch-angle scattering} \\ \alpha = 1 - \frac{1}{2} \beta_{\parallel} + \frac{1}{2} \beta_{\perp} \end{matrix}$$

Energetic particle distributions

- Solutions in the strong drive limit – balance between drive and loss
 - Typically heating time short compared with loss time
- Pressure of energetic particles rises until it is comparable to the remaining magnetic energy
 - Equipartition
 - Powerlaw solutions for the particle flux
 - Non-relativistic $j \sim p^2 f(p) \sim p^{-3} \sim E^{-1.5}$
 - Relativistic $j \sim E^{-2}$
- These distributions are the upper limits so that the energy integrals do not diverge
 - Harder spectra must have a limited range in energy

MeV electrons in a coronal hard x-ray source

- How to get MeV electrons in the corona?
 - A two-step process – heating in single x-line reconnection following by island merging
- First step: single x-line reconnection splits released energy between electrons, ions and bulk flow
 - $\beta_e \sim 1/4$
 - For $B \sim 50\text{G}$, with $n \sim 10^9\text{cm}^{-3}$, obtain $T_{\text{hot}} \sim 15\text{keV}$
- Second step: island mergers
 - Each merger doubles the electron energy – field line shortening
 - How many island mergers takes 10keV electrons to 1MeV?

$$15\text{keV} \times 2^N = 1\text{MeV} \Rightarrow N = 6$$

- Take typical island of size $W \sim 10^3\text{km}$
- Two island merging time $t_{\text{merge}} \sim (W/2)/0.1c_A \sim 1.5\text{s}$
- 1MeV electrons in $t_{1\text{MeV}} \sim 6t_{\text{merge}} = 9\text{s}$

Main Points

- Solar observations suggest that magnetic energy conversion into energetic electrons is extraordinarily efficient
- Fermi reflection and E_{\parallel} are the main drivers of electron acceleration during reconnection
 - First order rather than second order Fermi acceleration
 - Strong anisotropy of the energetic particle spectrum. What limits this anisotropy?
- Ion energy gain dominated by Fermi reflection
- Partitioning of electron and ion energy gain is not universal
 - An electric potential controls partitioning
 - Excellent agreement with magnetospheric satellite measurements
- Multi-x-line reconnection is required to produce the energetic component of the spectrum
 - Powerlaw spectra require a loss mechanism

Main Points

- The efficiency of energetic electron production in 3D increases dramatically compared with 2D
 - Electrons can wander throughout the reconnecting domain to access sites of magnetic energy release
 - No longer trapped within relaxed (contracted) magnetic islands as in 2D
- How are electrons confined within finite size regions where magnetic energy is being dissipated?
 - Their transit time is much shorter than their energy gain time
- Heated and energetic particles feed back magnetic energy release through the pressure anisotropy

$$p_{\parallel} > p_{\perp}$$

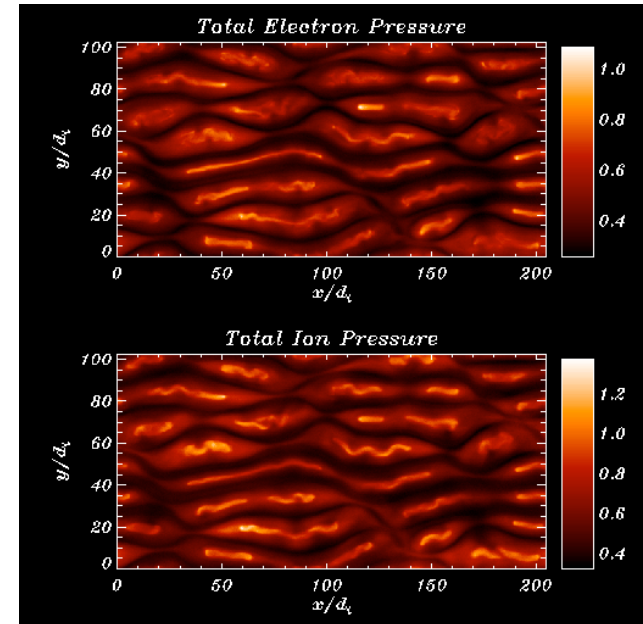
- Reduction of the field line tension that drives reconnection
- At the marginal firehose condition have no reconnection drive

The Feedback Problem

- Identifying the feedback of energetic particles on reconnection dynamics is essential
 - Test particles evolved in fields from 3-D MHD reconnection simulations rapidly exceed available magnetic energy (Onofri et al '06)
 - The energetic electrons approach β unity in solar flares (Krucker et al '10)
- Particles circulating in magnetic island undergo repeated Fermi reflections increase the parallel pressure until they hit the firehose stability boundary
- Magnetic fields have no tension at the marginal firehose condition

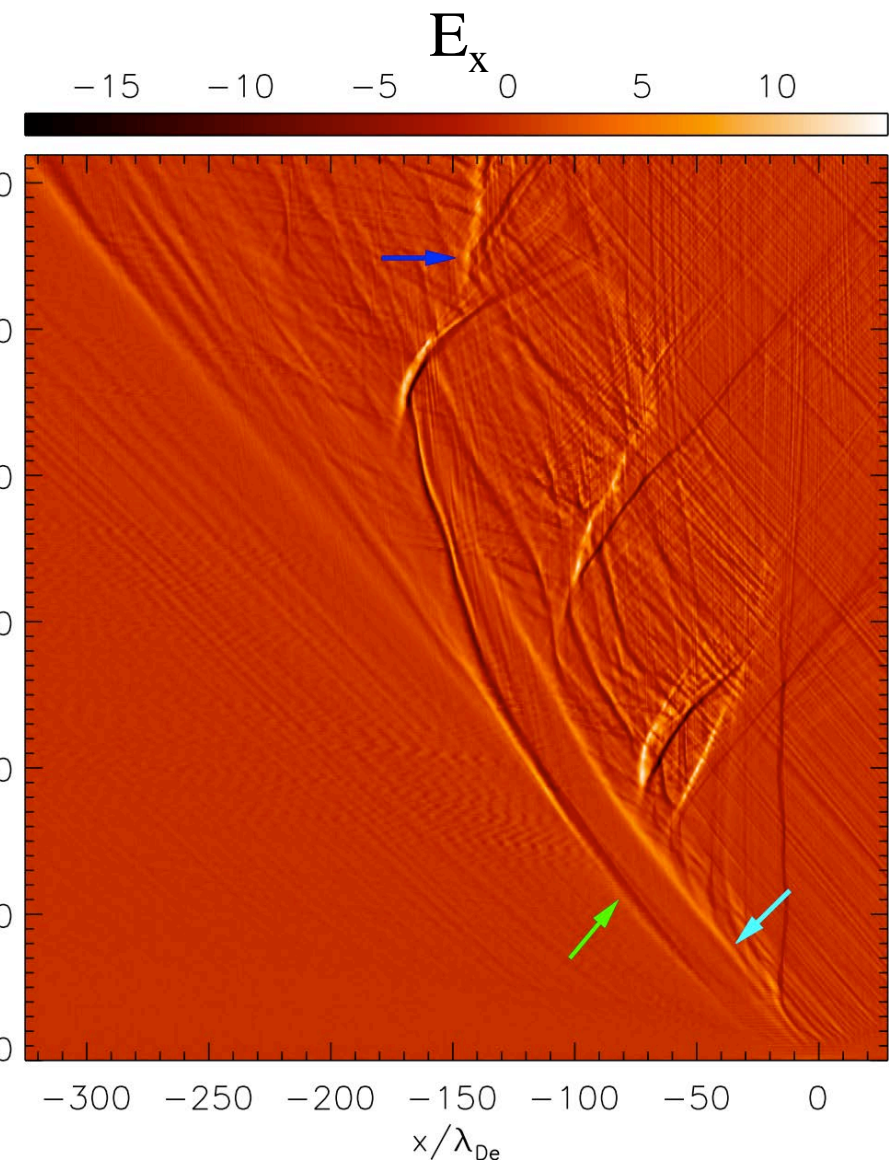
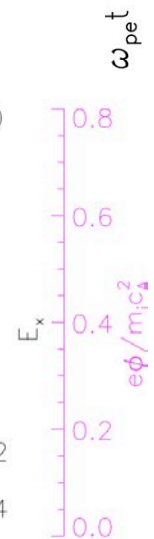
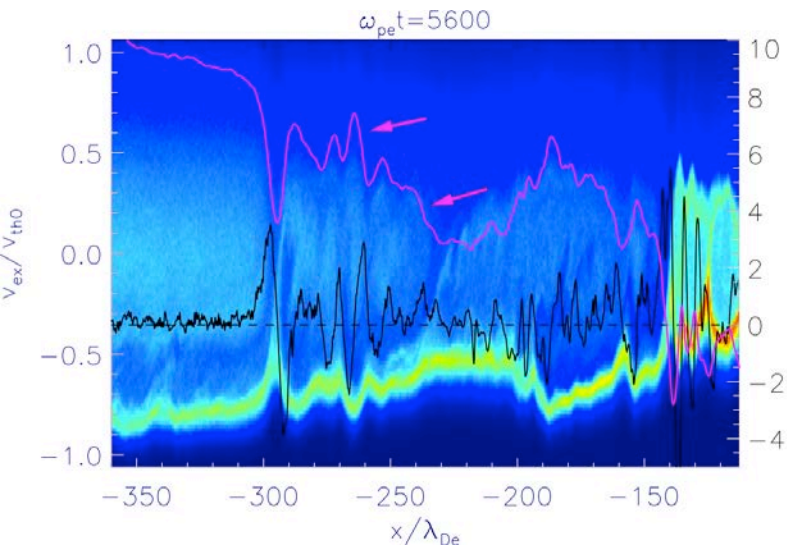
$$\omega^2 = k_{\parallel}^2 c_A^2 \left(1 - \frac{\beta_{\parallel}}{2} + \frac{\beta_{\perp}}{2} \right)$$

- Reconnection is throttled since tension drives reconnection



Suppression of electron heat flux by double layers

- Initialize a system with a localized region of high electron temperature
 - Hot electrons stream outward
 - High flux of return current electrons drives the Buneman instability
 - Development of double layers – localized region of intense parallel electric field
 - Strong suppression of electron transport



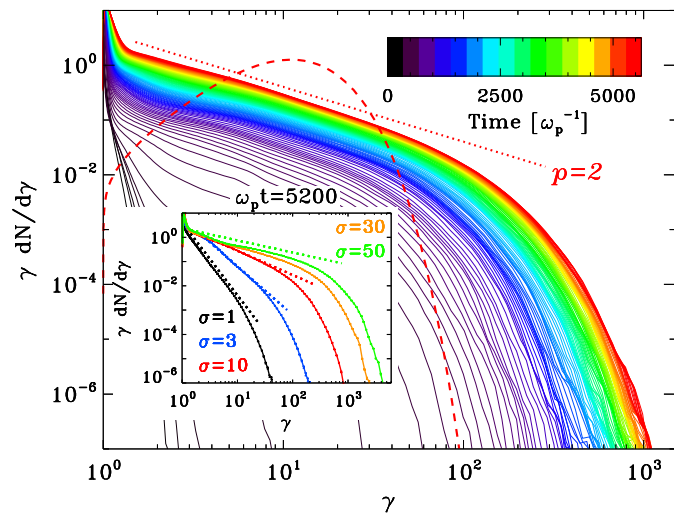
Li et al 2014

Powerlawspectra from reconnection

- Under what conditions do we expect powerlaws during reconnection?
 - With electron-proton reconnection in non-relativistic regime in periodic systems do not see powerlaws
 - Need loss mechanism to balance source to obtain powerlaws?
- Powerlaws develop in magnetically dominated plasmas. Why?

$$\sigma = B^2 / 4\pi n(m_i + m_e)c^2 \gg 1$$

- Powerlaws with indices $p < 2$ must have limited range in energy so the total integrated energy remains finite
 - Does a limited range powerlaw with index $p < 2$ make sense?



Sironi & Spitkovsky '14

An upper limit on energy gain during reconnection

- Magnetic reconnection dominantly increases the parallel energy of particles, depending on the degree of magnetization
 - Traditional limits in which particle energy gain is balanced by synchrotron loss yield upper limits on photons of around 160MeV
 - Photon energies above this are seen in the Crab flares
 - Spectral anisotropy can change these limits
- A true upper limit on energy comes from a balance between the energy gain due to the magnetic slingshot ($\sim \gamma/R$) and the particle radiation due to its motion along the curved field line ($\sim \gamma^4/R^2$)

$$\gamma < (R / R_c)^{1/3}$$

- Where $R_c = e^2 / mc^2$ is the classical electron radius and R is the field line radius of curvature.
- For the Crab flares this limit yields electron energies of 10^{15}eV